

Witnessing Entanglement without Entanglement Witness Operators

Luca Pezzè,¹ Yan Li,² Weidong Li,² and Augusto Smerzi¹

¹*QSTAR, INO-CNR and LENS, Largo Enrico Fermi 2, 50125 Firenze, Italy*

²*Institute of Theoretical Physics and Department of Physics, Shanxi University, 030006, Taiyuan, China*

(Dated: March 2, 2016)

Quantum mechanics predicts the existence of correlations between composite systems that, while puzzling our physical intuition, enable technologies not accessible in a classical world. Notwithstanding, there is still no efficient general method to theoretically quantify and experimentally detect entanglement of many qubits. Here we propose to detect entanglement by measuring the statistical response of a quantum systems to an arbitrary nonlinear parametric evolution. As a major difference with respect to current approaches based on the implementation of entanglement witness operators, we witness entanglement without relying on measurement efficiencies or tomographic reconstructions of the quantum state. The protocol requires only two collective settings for any number of parties. To illustrate its user-friendliness we demonstrate multipartite entanglement in different experiments with ions and photons by analyzing published data on fidelity visibilities and variances of collective observables.

A central problem in quantum technologies is to detect and characterize entanglement among correlated parties [1–3]. On the experimental side, the challenge is to certify entanglement in presence of imperfect measurements and decoherence due to the interaction of the system with the environment. A most popular approach is based on the implementation of entanglement witness operators (EWOs). An EWO is a Hermitian operator \mathcal{W} such that $\text{Tr}[\rho_{\text{sep}}\mathcal{W}] \geq 0$ for all separable states ρ_{sep} , and $\text{Tr}[\rho\mathcal{W}] < 0$ for, at least, one entangled state ρ [4–8]. The power of this method relies on the algebraic fact that for each multipartite entangled state it exists (at least) one EWO that recognizes it [4]. The experimental protocol implements projective measurements with the eigenvectors of \mathcal{W} so to directly extract $\text{Tr}[\rho\mathcal{W}]$. A drawback is that EWOs are device-dependent: they require precise and non-trivial assumptions on the efficiencies and fidelities of the projective measurements. In practice, experimental imperfections may easily lead to false positives, namely, to the unwitting realization of operators $\mathcal{W}_{\text{exp}} \neq \mathcal{W}$ such that $\text{Tr}[\rho_{\text{sep}}\mathcal{W}_{\text{exp}}] < 0$ also for (some) separable states, therefore signaling entanglement in states that are only classically correlated [9, 10]. The same problem arises, even more dramatically, when trying to detect entanglement via the tomographic reconstruction of the quantum state [10–12]. This problem has spurred an intense search for more robust entanglement witnesses criteria [13, 14].

A reliable experimental detection of entanglement requires the implementation of device-independent witness operators. An important class of entangled states is recognized by Bell-like inequalities testing the correlations between measurement data (obtained for different settings of non-communicating parties). These correlations among noninteracting parties cannot be created by local operations and experimental imperfections. Bell-like tests can thus detect entanglement without relying on any hypothesis about the measurement actually performed, nor they need any specific assumption on the state like, for in-

stance, its Hilbert space dimension. Therefore, it has been suggested that Bell-like inequalities are device-independent entanglement witness (DIEW) operators [15] and have been applied to maximally entangled states [15–18] of N qubit systems. Generally speaking, DIEWs demand that the parties i) must be addressed locally and ii) do not interact during the local operations and measurements. Also, the choice of the local operations settings is not straightforward: the specific configurations required to witness entanglement are only known for particular cases. The extension to an arbitrary state can vary from computationally hard to prohibitive since it can increase exponentially with the number of qubits. A recent experiment with trapped ions [19] has exploited Bell-based DIEWs and demonstrated genuine multipartite entanglement up to 6 particles. Crosstalk among the parties affected the DIEW of larger systems [19].

In this manuscript we propose a novel approach to witness entanglement based on the statistical speed of a quantum system driven by an arbitrary nonlinear transformations, see Fig. 1. As in the case of Bell-based DIEWs, it is state-independent and free from any constraint on the measurement efficiencies. However, our method does not require local manipulations and measurements: it detects entanglement with collective transformations even in presence of cross-talking between any number of qubits. It also extends the detection of entanglement beyond the usual realm of Bell-like tests to general multivariate observables. In the particular case of linear transformations, the statistical speed detects k -partite entanglement [20–22]. As it will be explained in detail below, our approach is not fully device independent because it requires the experimental control of the collective transformation. Several experiments have shown the feasibility of controlled collective phase shifts with cold [23, 24] and ultracold atoms [25–27], ions [28–32], photons [33, 34] and superconducting circuits [35]. We therefore demonstrate, by just elaborating on pub-

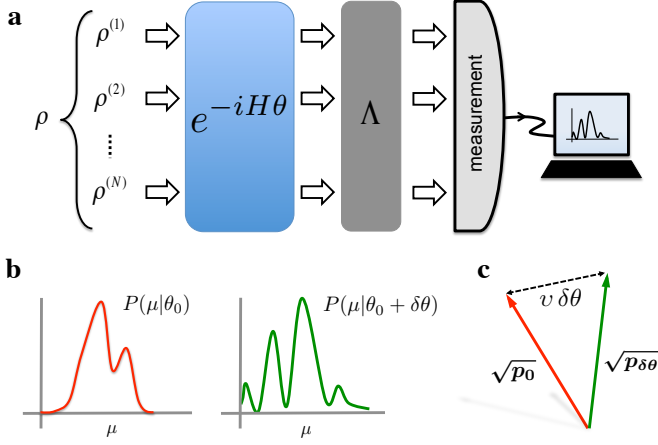


FIG. 1. **Statistical speed.** (a) N parties prepared in a quantum state ρ undergo a unitary transformation with θ a tunable parameter. The map Λ includes arbitrary θ -independent decoherence effects. (b) The probability distribution $P(\mu|\theta)$ is obtained by collecting the measurement results μ for different values of the parameter that here are chosen to be $\theta = \theta_0$ (red line) and $\theta = \theta_0 + \delta\theta$ (green line). (c). To quantify the statistical distinguishability between the two distributions we introduce unit vectors $\sqrt{p_0} = \{\sqrt{P(\mu|\theta_0)}\}_\mu$ (red) and $\sqrt{p_\theta} = \{\sqrt{P(\mu|\theta)}\}_\mu$ (green) and measure the Euclidean distance among them: $\ell \equiv 2\|\sqrt{p_0} - \sqrt{p_\theta}\|$ (dashed line). The statistical speed $v = \frac{d\ell}{d\theta}|_{\theta_0}$ is an entanglement witness.

lished experimental data [29, 30, 34, 36], entanglement up to 14 ions and 10 photons, and genuine multipartite entanglement up to 6 ions – in agreement with Bell-based DIEW results reported in Refs. [19]. This hallmarks the simplicity and interdisciplinary nature of our approach.

RESULTS

Witnessing entanglement via a statistical speed. Figure 1 illustrates the basic ingredients of our entanglement witness protocol. A quantum state ρ is probed by applying a collective transformation parametrized by a real number θ . The output state is characterized by the statistical probability distribution $P(\mu|\theta)$ of possible measurement results μ for a generic observable. The distinguishability between the two probability distributions $P(\mu|\theta_0)$ and $P(\mu|\theta)$ is quantified by the Hellinger distance [37]

$$\ell(\theta_0, \theta) = 2\sqrt{\sum_{\mu} \left(\sqrt{P(\mu|\theta_0)} - \sqrt{P(\mu|\theta)}\right)^2}, \quad (1)$$

with the sum extending over all possible measurement results μ . ℓ is a statistical distance [38, 39]: it ranges from zero, if and only if $P(\mu|\theta_0) = P(\mu|\theta) \forall \mu$, to its maximum value $\ell = 2\sqrt{2}$, if and only if $P(\mu|\theta_0) \times P(\mu|\theta) = 0 \forall \mu$, and it satisfies the

triangular inequality. The Hellinger distance is proportional to the Euclidean distance $\|\sqrt{p_0} - \sqrt{p_\theta}\|$ between the unit vectors $\sqrt{p_0} = \{\sqrt{P(\mu|\theta_0)}\}_\mu$ and $\sqrt{p_\theta} = \{\sqrt{P(\mu|\theta)}\}_\mu$. It is useful to introduce the notion of statistical speed: $v \equiv v(\theta_0) = \frac{d\ell}{d\theta}|_{\theta_0}$, i.e. the rate at which $\ell(\theta_0, \theta)$ changes with θ around the reference point θ_0 . A Taylor expansion of Eq. (1) gives

$$v^2 = \sum_{\mu} \frac{1}{P(\mu|\theta_0)} \left(\frac{dP(\mu|\theta)}{d\theta} \Big|_{\theta_0} \right)^2. \quad (2)$$

The squared statistical speed coincides with the “classical” Fisher information [40]. The specific measurement observable entering in Eqs. (1) and (2) via the conditional probabilities is arbitrary but, in practice, chosen so to efficiently distinguish the two probability distributions. Extracting the statistical speed requires (at least) two settings, independently from the number of particles, the quantum state and the measurement observable. Equation (2) is bounded by the quantum statistical speed $v^2 \leq v_Q^2 = \text{Tr}[\rho L^2]$, where L is the symmetric logarithmic derivative (SLD) uniquely defined on the support of ρ via the relation $\frac{d\rho}{d\theta} = \frac{L\rho + \rho L}{2}$ [38, 40]. For any quantum state, the bound can be saturated by optimal measurements [38]. Recently, it has been shown that the quantum statistical speed is linked to the dynamic susceptibility [41] and it is thus readily available in condensed-matter experiments.

Let us consider N qubits and apply the unitary transformation $e^{-iH\theta}$ (see Fig. 1), where

$$H = \sum_{i=1}^N \frac{\alpha_i}{2} \sigma_m^{(i)} + \varepsilon \sum_{i,j=1}^N \frac{V_{ij}}{4} \sigma_n^{(i)} \sigma_n^{(j)}, \quad (3)$$

coefficients α_i (without loss of generality, $0 \leq \alpha_i \leq 1$) account for (possibly) inhomogeneous linear couplings or local/subgroups operations on the parties, $V_{ij} = V_{ji}$ and ε is an arbitrary real number. Here, $\sigma_n^{(i)} \equiv \hat{\sigma}^{(i)} \cdot \mathbf{n}$ is the Pauli matrix for the i th particle and \mathbf{n} is a versor. What is the highest statistical speed obtained over all classically correlated states? The bound

$$v^2(\varepsilon) \leq \max_{|\psi_{\text{pr}}\rangle} v_Q^2(\varepsilon) \equiv v_{\text{max}}^2(\varepsilon) \quad (4)$$

holds, where the maximum of the quantum statistical speed is taken over all pure product state, $|\psi_{\text{pr}}\rangle = |\psi^{(1)}\rangle \otimes \dots \otimes |\psi^{(N)}\rangle$. As derived in Appendix, the quantum statistical speed of $|\psi_{\text{pr}}\rangle$ probed by the Hamiltonian H is

$$v_Q^2(\varepsilon) = v_0^2 + \varepsilon v_1^2 + \varepsilon^2 v_2^2, \quad (5)$$

where

$$v_0^2 = \sum_{i=1}^N \alpha_i^2 (1 - \langle \sigma_m^{(i)} \rangle^2), \quad (6)$$

$$v_1^2 = 2 \sum_{\substack{i,j=1 \\ i \neq j}}^N V_{ij} \alpha_i [\mathbf{n} \cdot \mathbf{m} - \langle \sigma_n^{(i)} \rangle \langle \sigma_m^{(i)} \rangle] \langle \sigma_n^{(j)} \rangle, \quad (7)$$

and

$$v_2^2 = \sum_{\substack{i,j=1 \\ i \neq j}}^N \frac{V_{ij}^2}{2} [1 - \langle \sigma_n^{(i)} \rangle^2 \langle \sigma_n^{(j)} \rangle^2] + \sum_{\substack{i,j,l=1 \\ i \neq j \neq l}}^N V_{ij} V_{il} [1 - \langle \sigma_n^{(i)} \rangle^2] \langle \sigma_n^{(j)} \rangle \langle \sigma_n^{(l)} \rangle. \quad (8)$$

Because of the convexity of the Fisher information [20], the bound $v^2(\varepsilon) \leq v_{\max}^2(\varepsilon)$ holds not only for pure states but also for any statistical mixture of product states (i.e. for an arbitrary classically-correlated state).

As $v_{\max}(\varepsilon)$ bounds the statistical speed over all possible observables and all separable states, states violating the inequality (4) are entangled. For linear Hamiltonians ($\varepsilon = 0$) the maximization is readily done: the optimal states have $\langle \sigma_n^{(i)} \rangle = 0 \forall i$, giving $v_{\max}^2(0) = \sum_{i=1}^N \alpha_i^2$. This generalizes the bound $v_{\max}^2(0) = N$ discussed in [20] for homogeneous coupling $\alpha_i = 1$. For nonlinear Hamiltonians ($\varepsilon \neq 0$) the bound depends on the explicit form of V_{ij} and α_i . It can be calculated either numerically or, as shown below, analytically in many cases of interest. In the following we consider, as an example, the Ising model having nearest-neighbor interaction $V_{ij} = \frac{\delta_{j,i+1} + \delta_{j,i-1}}{2}$ and $\mathbf{n} \cdot \mathbf{m} = 1$. In Appendix we also report the results for the Lipkin-Meshkov-Glick (LMG) model where $V_{ij} = 1$.

The states that maximize Eq. (5) are

$$|\psi(\varepsilon)\rangle = \prod_{i=1}^N \sqrt{\frac{1 + \langle \sigma_n^{(i)} \rangle}{2}} |\uparrow\rangle_i + e^{-i\varphi_i} \sqrt{\frac{1 - \langle \sigma_n^{(i)} \rangle}{2}} |\downarrow\rangle_i \quad (9)$$

where $|\uparrow\rangle$ and $|\downarrow\rangle$ are eigenstates of σ_n , φ_i are arbitrary phases and $\langle \sigma_n^{(i)} \rangle$ as a function of ε is reported in Fig. 2(a). Figure 2(b) shows $v_{\max}^2(\varepsilon)$ as a function of ε . The numerical analysis in the homogeneous case $\alpha_i = 1$ reveals that, for ε smaller than a critical value ε_c , the speed v_Q^2 is maximized when $\langle \sigma_n^{(i)} \rangle$ are all equal. In particular, for $\varepsilon \ll 1$, v_Q^2 is the highest when $\langle \sigma_n^{(i)} \rangle = \varepsilon \forall i$, giving $\frac{v_{\max}^2(\varepsilon)}{N} = 1 + \frac{5}{4}\varepsilon^2 + O(\varepsilon^4)$ (solid blue line in Fig. 2b). The value $\varepsilon_c = 0.7302$ is found analytically, as discussed in Appendix. For $\varepsilon > \varepsilon_c$, $v_Q^2(\varepsilon)$ is maximized by alternating $\langle \sigma_n^{(i)} \rangle = 1$ and $\langle \sigma_n^{(i+1)} \rangle = 0$. In this limit, we find $\frac{v_{\max}^2(\varepsilon)}{N} = \frac{1}{2} + \varepsilon + \frac{1}{2}\varepsilon^2$ (solid blue line in Fig. 2b). An upper bound to $v_{\max}^2(\varepsilon)$, valid in the inhomogeneous case ($\alpha_i \neq 0$) and for every ε , can be obtained by maximizing each term in Eq. (5) separately. This gives

$$v_{\max}^2(\varepsilon) \leq \sum_{i=1}^N \alpha_i^2 + \varepsilon \max \left(\sum_{\text{odd } i} \alpha_i, \sum_{\text{even } i} \alpha_i \right) + \varepsilon^2 \frac{N}{2}, \quad (10)$$

which is shown as dashed red line in Fig. 2b.

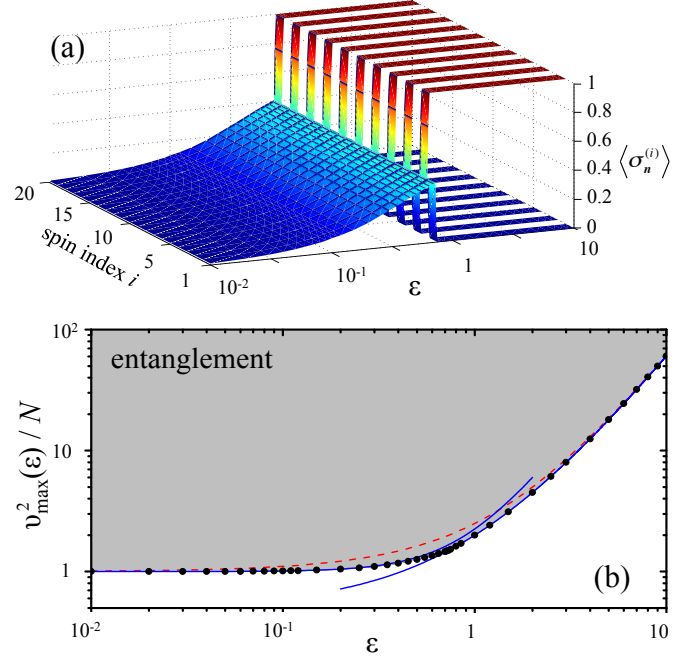


FIG. 2. **Witness of entanglement with the Ising Hamiltonian.** (a) Mean spin values $\langle \sigma_n^{(i)} \rangle$ for the separable states maximizing v_Q^2 , as a function of ε . (b) Maximum statistical speed of separable states, v_{\max}^2 (dots), probed by the Ising Hamiltonian. Entanglement is witnessed by a statistical speed $v^2 > v_{\max}^2$, i.e. in the grey region. The solid blue lines are analytical limits discussed in the main text. The dashed line is the upper bound Eq. (10).

It is important to emphasize that different Hamiltonians H detect different subsets of entangled states. Linear Hamiltonians ($\varepsilon = 0$) are well suited to detect entangled symmetric states. Entangled non-symmetric states are better detected by nonlinear Hamiltonians ($\varepsilon \neq 0$). Let's consider, for instance, the state of N spins $|\chi\rangle = (|\uparrow\downarrow\rangle^{\otimes N/2} + |\uparrow\rangle^{\otimes N/2} |\downarrow\rangle^{\otimes N/2})/\sqrt{2}$. It is possible to demonstrate that, when applying $e^{-iH_0\theta}$ with $H_0 = \frac{1}{2} \sum_{i=1}^N \sigma_n^{(i)}$, the quantum speed of $|\chi\rangle$ is smaller than the bound $v_{\max}^2 = N$ for $N > 6$, even when optimizing the direction \mathbf{n} . Therefore, $|\chi\rangle$ cannot be detected as entangled when probed by only linear Hamiltonians. Conversely, when probed by a nonlinear nearest-neighbor Hamiltonian $H_1 = \frac{1}{4} \sum_{i=1}^N \sigma_n^{(i)} \sigma_n^{(i+1)}$, this state has a square quantum statistical speed equal to $N^2/4 - N + 1$ that surpasses the bound $v_{\max}^2 = N/2$ if $N \geq 6$. $|\psi\rangle$ can thus be detected as entangled when probed by the Ising Hamiltonian. The opposite is also true. For instance the Greenberger-Horne-Zeilinger (GHZ) state $|\varphi\rangle = (|\uparrow\rangle^{\otimes N} + |\downarrow\rangle^{\otimes N})/\sqrt{2}$ has a null statistical speed when probed with H_1 . Nevertheless $|\varphi\rangle$ can reach a statistical speed $N^2 > N$ and it can thus be detected as entangled when probed by the linear Hamiltonian $H_0 = \frac{1}{2} \sum_{i=1}^N \sigma_n^{(i)}$.

Beside the possibility to witness a larger class of entangled

states, the measurement of the statistical speed generated by nonlocal Hamiltonians allows to take in account the residual coupling among neighboring spins that, in contrast, can limit the experimental implementation of Bell-based DIEWs, in particular when dealing with a large number of ions [19]. It is also important to notice that the bound (4) is not violated (no false positives are possible) if the state after the unitary transformation is affected by noise and decoherence (see Fig. 1) that, in full generality, can be modeled as a completely-positive trace-preserving map Λ [42, 43], when Λ does not depend on θ .

APPLICATIONS

Our method to witness entanglement requires to experimentally extract the statistical speed. We show below that this can be obtained from the visibility of fringe oscillating as a function of θ , from moments of the probability distribution or, more generally, by exploiting a basic relation between the statistical speed and the Kullback-Leibler entropy. We apply our protocols to extract the statistical speed from published data in ions and photons experiments. In these experiments, the probing Hamiltonian is linear and the above method can be extended as a witness of multiparticle entanglement [21, 22]: the inequality

$$v^2 > sk^2 + r^2, \quad (11)$$

signals $(k+1)$ -partite entanglement (i.e. among N parties, at least k are entangled), where s is the largest integer smaller than or equal to N/k and $r = N - sk$. In particular $v^2 > (N-1)^2 + 1$, obtained from Eq. (11) with $k = N-1$, is a witness of genuine N -partite entanglement.

Statistical speed from dichotomic measurements. We consider here the simplest (but experimentally relevant) case where the measurement results can only take two values, $\mu = \pm 1$. In this case, Eqs. (1) and (2) simplify to $\ell^2 = 8[1 - \sqrt{P_0 P_{\delta\theta}} - \sqrt{(1-P_0)(1-P_{\delta\theta})}]$ and

$$v^2 = \frac{1}{P_0(1-P_0)} \left(\frac{\partial P_\theta}{\partial \theta} \Big|_{\theta_0} \right)^2, \quad (12)$$

respectively, where $P_0 \equiv P(+1|\theta_0)$ and $P_{\delta\theta} \equiv P(+1|\theta_0 + \delta\theta)$. For instance, if

$$P(\pm 1|\theta) = \frac{1 \pm V \cos N\theta}{2}, \quad (13)$$

where V is the visibility, we can straightforwardly calculate Eq. (12), obtaining

$$v^2 = \frac{V^2 N^2 \sin^2(N\theta)}{1 - V^2 \cos^2(N\theta)}. \quad (14)$$

It is thus possible to detect entanglement when $V > \frac{1}{\sqrt{N}}$. Notice that, with an increasing number of qubits N the required minimum visibility to detect entanglement decreases. Maximally entangled states are detected when $V > \sqrt{(1 - \frac{1}{N})^2 + \frac{1}{N^2}}$, that requires a visibility increasing with N .

Statistical speed from average moments. Not always the probability of different measurement results are available, but only some averaged moments $\langle \mu \rangle_\theta = \sum_\mu \mu P(\mu|\theta)$. We can extend the notion of Hellinger distance and statistical speed to the probability distribution $P(\bar{\mu}|\theta)$, where $\bar{\mu} = \frac{1}{m} \sum_{i=1}^m \mu_i$ and μ_1, \dots, μ_m are measurement results. We find $\ell_{\text{mom}}^2 = 4 \sum_{\bar{\mu}} (\sqrt{P(\bar{\mu}|\theta_0)} - \sqrt{P(\bar{\mu}|\theta_0 + \delta\theta)})^2$ and

$$v_{\text{mom}}^2 = \sum_{\bar{\mu}} \frac{1}{P(\bar{\mu}|\theta_0)} \left(\frac{dP(\bar{\mu}|\theta)}{d\theta} \Big|_{\theta_0} \right)^2, \quad (15)$$

where the sum extends over all possible values of $\bar{\mu}$. Using a Cauchy-Schwarz inequality it is possible to demonstrate (see Appendix) that $v_{\text{mom}} \leq v\sqrt{m}$. For $m \gg 1$, the central limit theorem provides

$$P(\bar{\mu}|\theta) = \sqrt{\frac{m}{2\pi(\Delta\mu)_\theta^2}} e^{-\frac{m(\bar{\mu} - \langle \mu \rangle_\theta)^2}{2(\Delta\mu)_\theta^2}}, \quad (16)$$

where $(\Delta\mu)_\theta^2 = \sum_\mu (\mu - \langle \mu \rangle_\theta)^2 P(\mu|\theta)$. To the leading order in m , replacing Eq. (16) into Eq. (15), we obtain

$$v_{\text{mom}}^2 = \frac{m}{(\Delta\mu)_\theta^2} \left(\frac{d\langle \mu \rangle_\theta}{d\theta} \Big|_{\theta_0} \right)^2. \quad (17)$$

The entanglement criteria thus becomes $v_{\text{mom}}^2/m > v_H^2$. When probing with linear Hamiltonians, the inequality $v_{\text{mom}}^2/m > sk^2 + r^2$ witness $(k+1)$ -partite entanglement from the experimental measurements of average moments. These bounds generalize to arbitrary observables the bounds to detect entanglement [44] and multipartite entanglement [45] from the estimation of the mean collective spin [46, 47].

Witnessing multipartite entanglement in trapped-ions experiments. Several recent efforts have been devoted to create a GHZ state $\frac{1}{\sqrt{2}}(|0\rangle^{\otimes N} + |1\rangle^{\otimes N})$ with trapped ions [28–30]. In Ref. [28] the creation of the state has been followed by a collective rotation $\otimes_{j=1}^N e^{i\frac{\pi}{2}\sigma_\theta^{(j)}}$, with $\sigma_\theta^{(j)} = \sigma_x^{(j)} \cos \theta + \sigma_y^{(j)} \sin \theta$. The output state has been characterized by dichotomic measurements of the parity, $\Pi = (-1)^{N_0}$, with N_0 being the number of qubits measured in one of the two modes. The reported results are the oscillations of the average parity (and, therefore, of the probability to obtain the ± 1 result) as a function of θ , cfr.

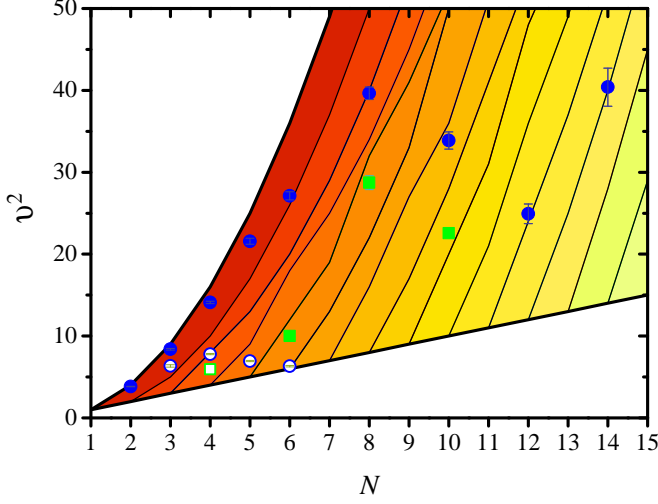


FIG. 3. **Witness of multipartite entanglement.** Squared statistical speed as a function of the number of qubits obtained analyzing published ions (circles) and photon (squares) experimental data: Ref. [28], filled circles; Ref. [29] for $N = 3$ and Ref. [30] for $N = 4, 5, 6$, open circles; Ref. [34], filled squares; Ref. [36], open square. The upper thick line is the upper bound $v^2 = N^2$, the lower thick line is the separability bound $v^2 = N$. The different lines are bound for k -partite entanglement, Eq. (11). In particular, the darker red region stands for genuine N -partite entanglement.

Eq. (13), and we can directly analyze the experimental data with our multipartite entanglement witness. In Fig. 3, filled blue circles are obtained from data reported in Ref. [28], for $N = \{2, 4, 6, 8, 10, 12, 14\}$, open blue circles from the data of Ref. [29] for $N = 3$ and of Ref. [30] for $N = 4, 5, 6$. We first notice that all data satisfy $v^2 > N$: we thus detect entanglement in *all the states* created in [28–30]. The different colored regions correspond to different k -partite entanglement detection [delimited by solid thin lines given by Eq. (11)]. In particular, genuine N -partite entanglement is marked by the darker red region that, from the data of Ref. [28], is reached up to $N = 6$ ions. The maximum value of v^2 is obtained for $N = 8$ particles, corresponding to 7-partite entanglement. The number of entangled particles in the system slowly decreases for increasing N : we have 4-partite entanglement for the states of $N = 10$ ions and 3-partite entanglement for the state of $N = 12$ and $N = 14$ ions. It is interesting to notice that a recent experiment [19] has investigated a Bell-based DIEW reporting genuine multipartite entanglement up to $N = 6$ ions, which is in agreement with our finding. We finally point out that our entanglement witness criteria do not assume any specific state, in particular, not necessarily GHZ-like [32].

Witnessing multipartite entanglement in photon experiments. Several experiments have demonstrated the creation of

multipartite entanglement in photonic systems [33, 34, 48, 49]. In particular, Ref. [34] reports on the creation of a GHZ states up to ten photons. After the creation of the state by parametric down-conversion, a phase shift is applied to each qubit, according to the scheme of Fig. 1. The state is finally characterized by measuring the operator $\sigma_x^{\otimes N}$, whose mean value shows high-frequency oscillations, $\langle \sigma_x^{\otimes N} \rangle = V \cos N\theta$ [34]. Noticing that $(\Delta \sigma_x^{\otimes N})^2 = 1 - \langle \sigma_x^{\otimes N} \rangle^2$, we can calculate the corresponding statistical speed from Eq. (17) to obtain $\frac{v_{\text{mom}}^2}{m} = \frac{V^2 N^2 \sin^2(N\theta)}{1 - V^2 \cos^2(N\theta)}$. Also in this case, the witness of multipartite entanglement is solely based on the visibility of the interference signal. Results are shown in Fig. 3 (filled squares). We witness 4-partite entanglement for the state of $N = 8$ photons, giving the highest value of the statistical speed reached with photons. As v_{mom}^2 is a lower bound of Eq. (2), the filled squares in Fig. 3 are lower bound for multipartite entanglement.

Statistical speed from the Kullback-Leibler entropy. So far we have extracted the statistical speed by fitting the experimental probabilities of the different detection events. This simple approach can be implemented when the probabilities can be accurately fitted with a single parameter function, as in the ions and photons experiments discussed above. In general, it might be necessary to extract the statistical speed directly from the bare data without fitting the probability distribution. This can be done by experimentally estimating the Kullback-Leibler (KL) entropy [50]:

$$D_{\text{KL}} = \sum_{\mu} P(\mu|\theta_0) \ln \frac{P(\mu|\theta_0)}{P(\mu|\theta_0 + \delta\theta)}. \quad (18)$$

The KL entropy grows quadratically for small $\delta\theta$ with a coefficient proportional to the squared statistical speed (2), $D_{\text{KL}} = v^2 \delta\theta^2 / 2$. In Fig. 4(a) we illustrate the method using experimental data of Ref. [28]. We focus to the case $N = 8$ and calculate D_{KL} around $\theta_0 \approx \pi/(2N)$ according to Eq. (18). A quadratic fit provides $v^2 = 44.6 \pm 7.7$, in agreement with the result ($v^2 = 39.6 \pm 0.8$) obtained using Eq. (13), see Fig. 3. The large error bars are due to the finite sample statistics of the published data and can be reduced by increasing the sample size and concentrating the measurements around a few phase values (rather than for the whole 2π interval).

To supply to the lack of available experimental data and for illustration purposes, here we implement a numerical Monte Carlo analysis of Eq. (18) to evaluate the role of $\delta\theta$ and the sample size, taking, as a testing ground, the parity measurements with probability (13). In Fig. 4(b) we plot Eq. (18) in the case $N = 8$ and $V = 0.787$, around $\theta_0 \approx \pi/(2N)$. The figure shows that the quadratic behavior is obtained at sufficiently large $\delta\theta$, see also Appendix. For comparison, we also show the Hellinger distance as a function of $\delta\theta$ which can also be exploited to extract experimentally the Fisher information [25].

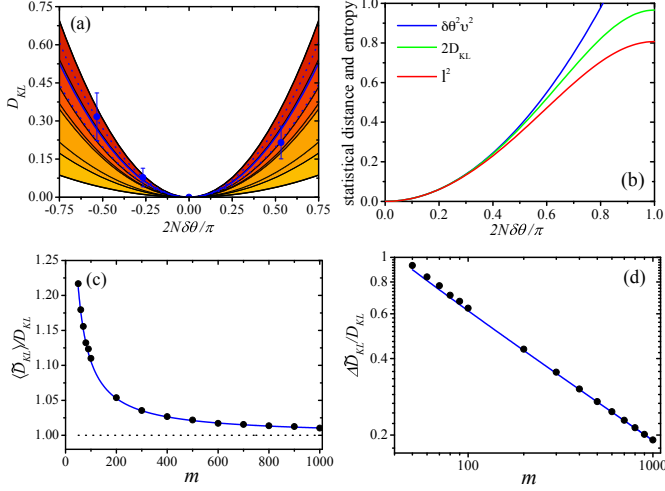


FIG. 4. **Kullback-Leibler entropy and statistical speed.** (a) KL entropy as a function of $\delta\theta$ obtained from an analysis of the experimental data of Ref. [28] for $N = 8$ ions. Blue dots are calculated using Eq. (18). The blue line is a parabolic fit, $D_{KL} = \delta\theta^2 v^2 / 2$. Color region corresponds to multipartite entanglement level, with color scale as in Fig. 3. (b) Squared statistical distance, ℓ^2 (red line), KL entropy, $2D_{KL}$ (green line), and their common low-order approximation, $\delta\theta^2 v^2$ (blue line), as a function of $\delta\theta$. Panels (c) and (d) reports numerical simulation of the Kullback-Leibler entropy (dots) as a function of the sample size m , for $2N\delta\theta/\pi = 0.4$. Solid lines are analytical predictions, valid for $m \gg 1$ (see text), for the statistical bias [in panel (c)] and the statistical fluctuation of D_{KL} [in panel (d)]. In panels (b)-(d) we used Eq. (13) for the probability, with $N = 8$ and $V = 0.787$, consistently with the experimental data of panel (a).

Notice that, for these values of the visibility, due to higher order terms (see Appendix) the quadratic approximation of D_{KL} holds at larger values of $\delta\theta$ than the ℓ^2 expansion.

A source of noise in the extraction of v^2 is the limited statistics of the measurement data (other sources of noise, as detection noise and decoherence, result in a reduced visibility). Let us indicate as m the sample size (we consider m measurements performed at phase θ_0 and m measurements performed at phase $\theta = \theta_0 + \delta\theta$). The experiment gives access to frequencies rather than probabilities, and Eq. (18) extends as $\tilde{D}_{KL} = f_0 \ln \frac{f_0}{f_{\delta\theta}} + (1 - f_0) \ln \frac{1-f_0}{1-f_{\delta\theta}}$, where $f_0 = n_{\text{even},0}/m$ is the frequency of even parity results obtained at phase θ_0 (and analogous definition for $f_{\delta\theta}$). Numerically, we can calculate f_0 and $f_{\delta\theta}$ by a Monte Carlo sampling of the probabilities P_0 and $P_{\delta\theta}$, respectively. In the large- m limit, we can calculate statistical fluctuations of the Hellinger distance by taking $f_0 = P_0 + \delta f_0$ and $f_{\delta\theta} = P_{\delta\theta} + \delta f_{\delta\theta}$, and then expanding \tilde{D}_{KL} in Taylor series for small $\delta f_{\delta\theta}$. We calculate the bias of the squared Hellinger distance, $b \equiv \langle \tilde{D}_{KL} \rangle - D_{KL}$, where brackets indicate statistical averaging. In the Method section we show that the bias is positive but decreases as $b \sim 1/2m$ with the sample size m . Figure 4(c) shows a comparison be-

tween a numerical Monte Carlo analysis and the analytical prediction. Similarly, we can evaluate statistical fluctuations of the KL entropy, $\Delta^2 \tilde{D}_{KL} = \langle \tilde{D}_{KL}^2 \rangle - \langle \tilde{D}_{KL} \rangle^2$. We obtain $\Delta^2 \tilde{D}_{KL} \sim 1/m$, showing, also in this case, a scaling inversely proportional to the sample size. Details of our analytical calculations are reported in the Method section, a comparison with analytical calculations is shown in Figure 4(d). Overall, the simulations show that few hundred measurements are sufficient to extract v^2 with a small statistical bias and large signal-to-noise.

DISCUSSION

The statistical speed reveals and quantifies entanglement among N parties. This requires to probe a quantum state with a generic multi-qubit Hamiltonian. Our approach shares several important properties of the device-independent entanglement witness based on Bell tests. A non-optimal choice of measurement, a noisy implementation of the observable, or a coupling with a decoherence source affecting the quantum state do not lead to a false detection of entanglement. It is also not necessary to exactly characterize the Hamiltonian applied to each party: for instance, systematic errors in the direction of Pauli matrices are fully tolerated.

The distinguishing property of our protocol is its simplicity: both computationally – it does not need local optimizations depending on the quantum state – and experimentally – it does not require multiple configurations and local operations. It also includes generic nonlocal interactions due to experimental tuning or accidental crosstalk effects. The number of operations required to witness entanglement does not increase with the number of parties: the statistical speed is extracted from the knowledge of, at least, two probability distributions obtained at nearby values of θ .

We have witnessed k -partite and genuine N -partite entanglement with trapped ions and photons by just analyzing published data. In particular we have demonstrated genuine N -partite entanglement up to $N = 6$ ions in agreement with recent experimental DIEW investigations [19]. It should be noticed that not all entangled states are characterized by a statistical speed larger than all separable states, even in a noiseless scenario and optimizing over output measurements. Yet, the entangled states violating Eq. (4) are those (and only those) overcoming the maximum interferometric phase sensitivity limit achievable with separable states and a phase-encoding transformation $e^{-iH\theta}$. Similarly, not all entangled states can be recognized by a Bell inequality: there are (mixed) entangled states that satisfy all possible Bell's inequalities.

To conclude, we notice that several experiments have focused on the creation of GHZ qubit states because, in addition to their foundational interest and possible applications, they

are recognized by (theoretically) simple witness operators of genuine N -partite entanglement. The method discussed in this manuscript allows the experimental characterization of a larger class of (hopefully including more robust against decoherence) quantum states. Finally, our results show that entanglement can be detected even when the probing Hamiltonian H is nonlinear and therefore generates entanglement. This opens the way to study entanglement near quantum phase transition points by quenching the parameters of the governing many-body Hamiltonian.

ACKNOWLEDGEMENTS

This work was supported by the National Natural Science Foundation of China (Grant No. 11374197), the PCSIRT (Grant No. IRT13076), The Hundred Talent Program of Shanxi Province (2012).

APPENDIX

Derivation of Eqs. (5)-(8). For pure states and unitary transformation $e^{-i\theta H}$, the quantum statistical speed is given by $v_Q^2(\varepsilon) = 4(\Delta H)^2$. Taking $H = H_0 + \varepsilon H_1$, $v_Q^2(\varepsilon)$ is given by Eq. (5) with $v_0^2 = 4(\Delta H_0)^2$, $v_1^2 = 4(\langle\{H_0, H_1\}\rangle - 2\langle H_0\rangle\langle H_1\rangle)$ and $v_2^2 = 4(\Delta H_1)^2$. We detail here the calculation of v_2^2 for product pure states, where $H_1 = \sum_{i,j=1}^N \frac{V_{ij}}{4} \sigma_n^{(i)} \sigma_n^{(j)}$. We have $v_2^2 = \sum_{i,j,k,l} \frac{V_{ij}V_{kl}}{4} [\langle \sigma_n^{(i)} \sigma_n^{(j)} \sigma_n^{(k)} \sigma_n^{(l)} \rangle - \langle \sigma_n^{(i)} \sigma_n^{(j)} \rangle \langle \sigma_n^{(k)} \sigma_n^{(l)} \rangle]$. Notice that the terms $i \neq j$ and $k \neq l$ do not contribute to v_2^2 . For product states we thus have $\langle \sigma_n^{(i)} \sigma_n^{(j)} \rangle \langle \sigma_n^{(k)} \sigma_n^{(l)} \rangle = \langle \sigma_n^{(i)} \rangle \langle \sigma_n^{(j)} \rangle \langle \sigma_n^{(k)} \rangle \langle \sigma_n^{(l)} \rangle$ while $\langle \sigma_n^{(i)} \sigma_n^{(j)} \sigma_n^{(k)} \sigma_n^{(l)} \rangle = \langle \sigma_n^{(i)} \rangle \langle \sigma_n^{(j)} \rangle \langle \sigma_n^{(k)} \rangle \langle \sigma_n^{(l)} \rangle$ only if the indexes i, j, k, l are all different. Therefore, only terms where at least two indexes are equal contribute to v_2^2 . The terms $k = i, l = j$ and $k = j, l = i$ both contribute with $\sum_{i,j} \frac{V_{ij}^2}{4} (1 - \langle \sigma_n^{(i)} \rangle^2 \langle \sigma_n^{(j)} \rangle^2)$. After straightforward algebra, taking into account all contributing terms, one arrives at Eq. (8). Repeating the same procedure for v_0^2 and v_1^2 , where $H_0 = \sum_{i=1}^N \frac{\alpha_i}{2} \sigma_m^{(i)}$, one derives Eq. (5).

Statistical speed for the Ising model. We provide here details on the analysis of the Ising model discussed in the main text. We consider the homogeneous case $\alpha_i = 1$ and $n = m$. For $\varepsilon \leq \varepsilon_c$ we find numerically that $v_Q^2(\varepsilon)$ is maximized by taking the same $\langle \sigma_n^{(i)} \rangle$ for all $i = 1, \dots, N$, see Fig. (2). The optimization is thus done by replacing $\langle \sigma_n^{(i)} \rangle = a$ in Eqs. (5)

and (8). This provides the equation

$$\frac{v_Q^2(\varepsilon)}{N} = (1 - a^2) + 2\varepsilon(a - a^3) + \frac{\varepsilon^2}{4}(1 + 2a^2 - 3a^4) \quad (19)$$

that can be maximized over a at fixed value of ε . The exact analytical expression is long and not reported here. For $\varepsilon \ll 1$ we find $a = \varepsilon + O(\varepsilon^3)$, giving $\frac{v_{\max}^2(\varepsilon)}{N} = 1 + \frac{5}{4}\varepsilon^2 + O(\varepsilon^4)$. For $\varepsilon > \varepsilon_c$ we obtain numerically that $v_Q^2(\varepsilon)$ is maximized when $\langle \sigma_n^{(i)} \rangle = 1$ and $\langle \sigma_n^{(i)} \rangle = 0$, giving

$$\frac{v_{\max}^2(\varepsilon)}{N} = \frac{1}{2} + \varepsilon + \frac{\varepsilon^2}{2}. \quad (20)$$

Indeed, in the limit $\varepsilon \gg 1$, Eq. (20) goes as $\sim \varepsilon^2/2$ and thus overcomes Eq. (19), which goes as $\sim \varepsilon^2/3$ at best, as obtained by maximizing $(1 + 2a^2 - 3a^4)$ over a . The value of ε for which Eq. (20) is equal to the maximum over a of Eq. (19) defines the critical ε_c .

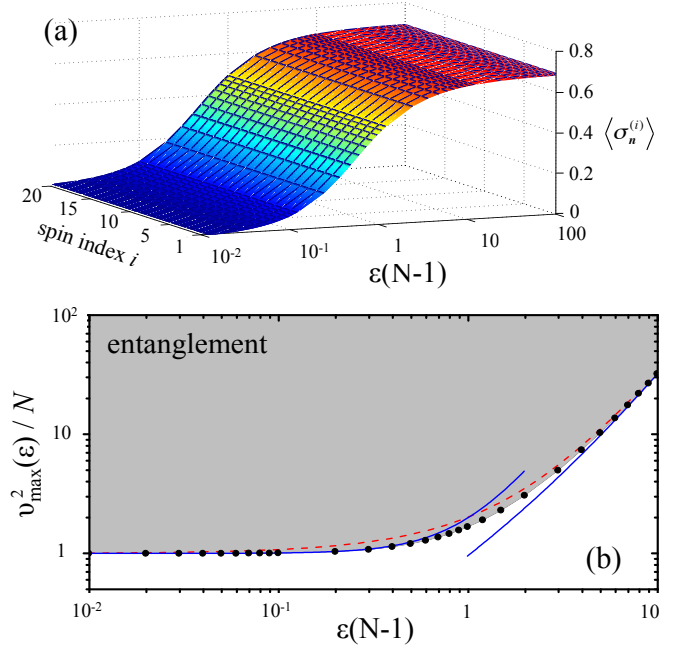


FIG. 5. Witness of entanglement with the LMG Hamiltonian. Same as Fig. 2 but calculated here for the LMG model $V_{ij} = 1$. (a) Mean spin $\langle \sigma_n^{(i)} \rangle$ of the optimal separable as a function of $\tilde{\varepsilon}$. In this case $\langle \sigma_n^{(i)} \rangle$ is the same for all spins. (b) Dots are the numerical optimization, the solid blue lines are Eq. (22) for $\tilde{\varepsilon} \equiv \varepsilon(N-1) \ll 1$ and Eq. (23) for $\tilde{\varepsilon} \gg 1$. The dashed line is the upper bound Eq. (24).

Statistical speed for the LMG model. We discuss here $v_{\max}^2(\varepsilon)$ for the LMG model. We consider the Hamiltonian (3) with $V_{ij} = 1$, $n = m$ and focus on the homogeneous case $\alpha_i = 0$. In this case, we numerically find that, for all values of

ε , $v_Q^2(\varepsilon)$ is maximized taking equal $\langle \sigma_n^{(i)} \rangle$ for all $i = 1, \dots, N$. Replacing $\langle \sigma_n^{(i)} \rangle = a$ in Eqs. (5) and (8) we find

$$\frac{v_Q^2(\varepsilon)}{N} = (1 - a^2) + 2\tilde{\varepsilon}a(1 - a^2) + \tilde{\varepsilon}^2 \frac{1 + 2(N-2)a^2 - (2N-1)a^4}{2(N-1)}, \quad (21)$$

where $\tilde{\varepsilon} = \varepsilon(N-1)$. This equation can be maximized over a analytically for each $\tilde{\varepsilon}$ and N (the explicit expression is long and not reported here). For $\tilde{\varepsilon} \ll 1$, we have $a = \tilde{\varepsilon}$ giving

$$\frac{v_{\max}^2(\varepsilon)}{N} = 1 + \tilde{\varepsilon}^2. \quad (22)$$

In the opposite $\tilde{\varepsilon} \gg 1$ limit, we find $a = \sqrt{\frac{N-2}{2N-1}}$ giving

$$\frac{v_{\max}^2(\varepsilon)}{N} = \tilde{\varepsilon}^2 \frac{(N-1)}{2(2N-3)} \quad (23)$$

Maximizing each term of Eq. (21) separately, we can find an upper bound to v_H^2 :

$$\frac{v_{\max}^2(\varepsilon)}{N} \leq 1 + \frac{4}{3\sqrt{3}}\tilde{\varepsilon} + \frac{(N-1)}{2(2N-3)}\tilde{\varepsilon}^2. \quad (24)$$

A comparison between numerical results, the limits (22) and (23), and the bound Eq. (24) is shown in Fig. 5.

Statistical speed for multiple measurements. We can extend the notion of Hellinger distance [given in Eq. (1) for a single measurement] to the case of m measurements:

$$\ell_m^2(\theta_0, \theta) = 8 \left[1 - \sum_{\mu} \sqrt{P(\mu|\theta_0)P(\mu|\theta)} \right],$$

where $P(\mu|\theta)$ is the probability to obtain the sequence $\mu \equiv \{\mu_1, \dots, \mu_m\}$ (μ_i is the result of the i th measurement) when the phase shift is equal to θ , and the sum runs over all possible sequences. For independent measurements we have $P(\mu_1, \dots, \mu_m|\theta) = \prod_{i=1}^m P(\mu_i|\theta)$, and $\ell_m^2(\theta_0, \theta)$ becomes

$$\ell_m^2(\theta_0, \theta) = 8 \left[1 - \left(\sum_{\mu} \sqrt{P(\mu|\theta)P(\mu|\theta_0)} \right)^m \right].$$

A Taylor expansion for $\theta \sim \theta_0$ gives $\ell_m^2 = mv^2(\theta - \theta_0)^2$. In the following we demonstrate that the inequalities

$$\ell_{\text{mom}}^2 \leq \ell_m^2, \quad \text{and} \quad v_{\text{mom}}^2 \leq mv^2$$

hold. To show this, let us rewrite the probability of $\bar{\mu}$ as

$$P(\bar{\mu}|\theta) = \sum_{\mu} \delta(\xi_m - \bar{\mu}) \prod_{i=1}^m P(\mu_i|\theta),$$

where $\xi_m = \frac{1}{m} \sum_{i=1}^m \mu_i$ and a Cauchy-Schwarz inequality gives

$$\sqrt{P(\bar{\mu}|\theta)P(\bar{\mu}|\theta_0)} \geq \sum_{\mu} \delta(\xi_m - \bar{\mu}) \prod_{i=1}^m \sqrt{P(\mu_i|\theta)P(\mu_i|\theta_0)}$$

Summing over $\bar{\mu}$, we conclude that

$$\begin{aligned} \ell_{\text{mom}}^2 &= 8 \left[1 - \sum_{\bar{\mu}} \sqrt{P(\bar{\mu}|\theta)P(\bar{\mu}|\theta_0)} \right] \\ &\leq 8 \left[1 - \left(\sum_{\mu} \sqrt{P(\mu|\theta)P(\mu|\theta_0)} \right)^m \right] = \ell_m^2, \end{aligned}$$

From a second-order Taylor expansion of both members around $\theta \sim \theta_0$, we obtain that $v_{\text{mom}}^2/m \leq v^2$.

Statistical bias and fluctuations of the Kullback-Leibler entropy. We calculate the statistical bias of the Kullback-Leibler entropy $b \equiv \langle \tilde{D}_{\text{KL}} \rangle - D_{\text{KL}}$. This is done analytically by replacing $f_\theta = P_\theta + \delta f_\theta$ into the definition of \tilde{D}_{KL} and performing a second-order Taylor expansion for $\delta f_\theta \ll P_\theta, 1 - P_\theta$ (we require here $P_\theta \neq 0, 1$). We use binomial statistics, such that $\langle \delta f_\theta \rangle = 0$, $\langle \delta f_\theta^2 \rangle = P_\theta[1 - P_\theta]/m$ and uncorrelated detection, $\langle \delta f_\theta \delta f_0 \rangle = 0$. We obtain

$$b = \frac{P_0}{2mP_{\delta\theta}} + \frac{1 - P_0}{2m(1 - P_{\delta\theta})}. \quad (25)$$

Following an analogous method, it is possible to calculate the statistical fluctuations of the KL entropy. To the leading order in m we have

$$(\Delta \tilde{D}_{\text{KL}})^2 = \frac{(P_0 - P_{\delta\theta})^2}{m(1 - P_{\delta\theta})P_{\delta\theta}} + \frac{(1 - P_0)P_0}{m} \ln^2 \frac{(1 - P_0)P_{\delta\theta}}{(1 - P_{\delta\theta})P_0}. \quad (26)$$

-
- [1] O. Gühne and G. Tóth. Entanglement detection. *Phys. Rep.* **474**, 1 (2009).
 - [2] R. Horodecki, P. Horodecki, M. Horodecki and K. Horodecki. Quantum entanglement. *Rev. Mod. Phys.* **81**, 865 (2009).
 - [3] L. Amico, R. Fazio, A. Osterloh and V. Vedral. Entanglement in many-body systems. *Rev. Mod. Phys.* **80**, 517 (2008).
 - [4] M. Horodecki, P. Horodecki and R. Horodecki. Separability of mixed states: necessary and sufficient conditions. *Phys. Lett. A* **223**, 1 (1996).
 - [5] M. Horodecki, P. Horodecki and R. Horodecki. Separability of n -particle mixed states: necessary and sufficient conditions in terms of linear maps. *Phys. Lett. A* **283**, 1 (2001).
 - [6] B.M. Tehral. Detecting quantum entanglement. *Theoretical Computer Science* **287** 313 (2002).
 - [7] M. Lewenstein, B. Kraus, J.I. Cirac and P. Horodecki. Optimization of entanglement witnesses. *Phys. Rev. A* **62**, 052310 (2000).
 - [8] J. Sperling and W. Vogel. Multipartite Entanglement Witnesses. *Phys. Rev. Lett.* **111**, 110503 (2013).

- [9] M. Seevinck and J. Uffink. Sufficient conditions for three-particle entanglement and their tests in recent experiments. *Phys. Rev. A* **65**, 012107 (2001).
- [10] D. Rosset, R. Ferretti-Schöbitz, J.-D. Bancal, N. Gisin and Y.-C. Liang. Imperfect measurement settings: Implications for quantum state tomography and entanglement witnesses. *Phys. Rev. A* **86**, 062325 (2012).
- [11] A.I. Lvovsky and M.G. Raymer. Continuous-variable optical quantum-state tomography. *Rev. Mod. Phys.* **81**, 299 (2009).
- [12] T. Moroder, M. Kleinmann, P. Schindler, T. Monz, O. Gühne and R. Blatt. Certifying Systematic Errors in Quantum Experiments. *Phys. Rev. Lett.* **110**, 180401 (2013).
- [13] M. Cianciaruso, T.R. Bromley and G. Adesso. Accessible quantification of multipartite entanglement. arXiv:1507.01600.
- [14] J.C. Loredó, M.P. Almeida, R. Di Candia, J.S. Pedernales, J. Casanova, E. Solano, and A.G. White. Measuring Entanglement in a Photonic Embedding Quantum Simulator. *Phys. Rev. Lett.* **116**, 070503 (2016).
- [15] J.-D. Bancal, N. Gisin, Y.-C. Liang and S. Pironio. Device-Independent Witnesses of Genuine Multipartite Entanglement. *Phys. Rev. Lett.* **106**, 250404 (2011).
- [16] M. Seevinck and G. Svetlichny. Bell-Type Inequalities for Partial Separability in N -Particle Systems and Quantum Mechanical Violations. *Phys. Rev. Lett.* **89**, 060401 (2002).
- [17] K. Nagata, M. Koashi and N. Imoto. Configuration of Separability and Tests for Multipartite Entanglement in Bell-Type Experiments. *Phys. Rev. Lett.* **89**, 260401 (2002).
- [18] K.F. Pál and T. Vértesi. Multisetting Bell-type inequalities for detecting genuine multipartite entanglement. *Phys. Rev. A* **83**, 062123 (2011).
- [19] J.T. Barreiro, J.-D. Bancal, P. Schindler, D. Nigg, M. Hennrich, T. Monz, N. Gisin and R. Blatt. Demonstration of genuine multipartite entanglement with device-independent witnesses. *Nat. Phys.* **9**, 559 (2013).
- [20] L. Pezzè and A. Smerzi. Entanglement, Nonlinear Dynamics, and the Heisenberg Limit. *Phys. Rev. Lett.* **102**, 100401 (2009).
- [21] G. Tóth. Multipartite entanglement and high-precision metrology. *Phys. Rev. A* **85**, 022322 (2012).
- [22] P. Hyllus, W. Laskowski, R. Krischek, C. Schwemmer, W. Wieczorek, H. Weinfurter, L. Pezzè and A. Smerzi. Fisher information and multipartite entanglement. *Phys. Rev. A* **85**, 022321 (2012).
- [23] J. Appel, P.J. Windpassinger, D. Oblak, U. B. Hoff, N. Kjaergaard and E.S. Polzik. Mesoscopic atomic entanglement for precision measurements beyond the standard quantum limit. *PNAS* **106**, 10960 (2009).
- [24] J.G. Bohnet, K.C. Cox, M.A. Norcia, J.M. Weiner, Z. Chen and J.K. Thompson. Reduced spin measurement back-action for a phase sensitivity ten times beyond the standard quantum limit. *Nat. Phot.* **8**, 731 (2014).
- [25] H. Strobel, et al. Fisher information and entanglement of non-Gaussian spin states. *Science* **345**, 424 (2014).
- [26] B. Lücke, et al. Twin Matter Waves for Interferometry Beyond the Classical Limit. *Science* **334**, 773 (2011).
- [27] M.F. Riedel, P. Böhi, Y. Li, T.W. Hänsch, A. Sinatra, and P. Treutlein. Atom-chip-based generation of entanglement for quantum metrology. *Nature* **464**, 1170 (2010).
- [28] T. Monz, P. Schindler, J.T. Barreiro, M. Chwalla, D. Nigg, W.A. Coish, M. Harlander, W. Hänsel, M. Hennrich and R. Blatt. 14-Qubit Entanglement: Creation and Coherence. *Phys. Rev. Lett.* **106**, 130506 (2011).
- [29] D. Leibfried, et al. Toward Heisenberg-Limited Spectroscopy with Multipartite Entangled States. *Science* **304**, 1476 (2005).
- [30] D. Leibfried, et al. Creation of a six-atom ‘Schrödinger cat’ state. *Nature* **438**, 639 (2006).
- [31] H. Häffner, et al., Scalable multipartite entanglement of trapped ions. *Nature* **438**, 643 (2005).
- [32] J.G. Bohnet, B.C. Sawyer, J.W. Britton, M.L. Wall, A.M. Rey, M. Foss-Feig and J.J. Bollinger. Quantum spin dynamics and entanglement generation with hundreds of trapped ions. arXiv:1512.03756.
- [33] X.-C. Yao, et al. Observation of eight-photon entanglement. *Nat. Phot.* **6**, 225 (2012).
- [34] W.-B. Gao, et al. Experimental demonstration of a hyper-entangled ten-qubit Schrödinger cat state. *Nat. Phys.* **6**, 331 (2010).
- [35] L. DiCarlo, et al. Preparation and measurement of three-qubit entanglement in a superconducting circuit. *Nature* **467**, 574 (2010).
- [36] P. Walther, J.-W. Pan, M. Aspelmeyer, R. Ursin, S. Gasparoni and A. Zeilinger. De Broglie wavelength of a non-local four-photon state. *Nature* **429**, 158 (2004).
- [37] I. Begtsso and K. Życzkowski. *Geometry of Quantum States: An Introduction to Quantum Entanglement* (Cambridge University Press, 2000).
- [38] S.L. Braunstein and C.M. Caves. Statistical Distance and the Geometry of Quantum States. *Phys. Rev. Lett.* **72**, 3439 (1994).
- [39] W.K. Wootters. Statistical distance and Hilbert space. *Phys. Rev. D* **23**, 357 (1981).
- [40] C.W. Helstrom. *Quantum detection and estimation theory*. (Academic Press, Oxford, 1976).
- [41] P. Hauke, M. Heyl, L. Tagliacozzo and P. Zoller. Measuring multipartite entanglement via dynamic susceptibilities. arXiv:1509.01739.
- [42] V. Giovannetti, S. Lloyd and L. Maccone. Quantum Metrology. *Phys. Rev. Lett.* **96**, 010401 (2006).
- [43] R. Demkowicz-Dobrzański, J. Kolodyński and M. Guta, The elusive Heisenberg limit in quantum-enhanced metrology. *Nat. Comm.* **3**, 1063 (2012).
- [44] A. Sørensen, L.-M. Duan, J.I. Cirac and P. Zoller. Many-particle entanglement with Bose-Einstein condensates. *Nature* **409**, 63 (2001).
- [45] A.S. Sørensen and K. Mølmer, Entanglement and Extreme Spin Squeezing. *Phys. Rev. Lett.* **86**, 4431 (2001).
- [46] D.J. Wineland, J.J. Bollinger, W.M. Itano, and D.J. Heinzen, Squeezed atomic states and projection noise in spectroscopy. *Phys. Rev. A* **50**, 67 (1994).
- [47] J. Ma, X. Wang, C.P. Sun and F. Nori, Quantum spin squeezing. *Phys. Rep.* **509**, 89 (2011).
- [48] Z. Zhao, Y.-A. Chen, A.-N. Zhang, T. Yang, H.J. Briegel and J.-W. Pan. Experimental demonstration of five-photon entanglement and open-destination teleportation. *Nature* **430**, 54 (2004).
- [49] D. Bouwmeester, J.-W. Pan, M. Daniell, H. Weinfurter and A. Zeilinger. Observation of Three-Photon Greenberger-Horne-Zeilinger Entanglement. *Phys. Rev. Lett.* **82**, 1345 (1999).
- [50] S. Kullback and R.A. Leibler. On information and sufficiency. *Ann. Math. Stat.* **22**, 79 (1951).